Channel Training for Analog FDD Repeaters: Optimal Estimators and Cramér-Rao Bounds

Stefan Wesemann and Thomas L. Marzetta
Bell Labs, Nokia
Email: stefan.wesemann@nokia-bell-labs.com, tlm@research.bell-labs.com

arXiv:1610.03260v1 [cs.IT] 11 Oct 2016

***Abstract*—A network of analog repeaters, each fed by a wireless fronthaul link and powered by e.g., solar energy, is a promising candidate for a flexible small cell deployment. A key challenge is the acquisition of accurate channel state information by the fronthaul hub (FH), which is needed for the spatial multiplexing of multiple fronthaul links over the same time/frequency resource. For frequency division duplex channels, a simple pilot loop-back procedure has been proposed that allows the estimation of the UL & DL channels at the FH without relying on any digital signal processing at the repeater side. For this scheme, we derive the maximum likelihood (ML) estimators for the UL & DL channel subspaces, formulate the corresponding Cramér-Rao bounds and show the asymptotic efficiency of both (SVD-based) estimators by means of Monte Carlo simulations. In addition, we illustrate how to compute the underlying (rank-1) SVD with quadratic time complexity by employing the power iteration method. To enable power control for the fronthaul links, knowledge of the channel gains is needed. Assuming that the UL & DL channels have on average the same gain, we formulate the ML estimator for the UL channel gain, and illustrate its robustness against strong noise by means of simulations.**

***Index Terms*—Analog feedback, fronthaul channel, frequency-division duplex, analog repeater, channel state information (CSI), wireless communication, multiple-input single-output (MISO)**

I. Introduction

ANALOG repeaters, driven by a wireless fronthaul and powered by e.g., solar energy, enable flexible and energy autonomous small cell deployments. Especially in frequency division duplex (FDD) systems, the repeater architecture is quite simple because the uplink (UL) and downlink (DL) channels are separated by bandpass filters, so that no transmit-receive switching is required. The resulting repeater architecture is illustrated in Figure 1, and is supposed to have a total power consumption of less than 15 Watts so that the repeater can be fed by a small size solar panel. In order to spatially multiplex multiple FDD fronthaul links over the same time/frequency resource (e.g., by means of Massive MIMO [1]), the fronthaul hub (FH) requires accurate channel state information (CSI). Classical channel training methods for FDD systems (e.g., [2], [3], [4], [5], [6], [7]), however, are not applicable because they rely on digital signal processing capabilities at the repeater side (e.g., transmission of pilots in the UL, estimation and feedback of the DL CSI). Therefore, a simple FDD channel training method has been proposed in [8] that requires only analog processing at the repeater side. The training of the individual repeaters is performed sequentially in time, which is justified by the observation that small cells are typically mounted on elevated locations (above the clutter). Consequently, we can expect relatively large channel coherence times in the order of 1/10s to 1s (see e.g., [9, Table III]). For each repeater, the channel training consists of the DL pilot transmission by the FH, and the immediate 'reflection' of the received pilot signal by the repeater in the UL of the fronthaul. In order to cope with frequency-selective channels, multiple pilot signals can be multiplexed in the frequency domain on quasi-flat subbands.

Given the received signal, the FH has to estimate both the UL & DL fronthaul channels. As shown in Section II, the received signal contains the (outer) product of the two unknown channels, so that each channel vector can be estimated only up to an unknown scalar scaling factor. The only observable invariants of the propagation channels are their subspaces. Therefore, we formulate in Section III the maximum likelihood (ML) estimators for the UL & DL subspaces. Based on the intrinsic Cramér-Rao bounds (CRB) derived in [10], we are able to lower bound the subspace estimation accuracy. In Section III-C, we discuss methods that allow a significant reduction of the subspace estimator's computational complexity, and evaluate these by means of Monte Carlo simulations in Section V. Moreover, assuming knowledge about the repeater's average transmit power and the UL perturbation variance, we formulate in Section IV the ML estimator for UL channel vector norm, which is needed for the power control of the fronthaul links. Finally, we summarize our findings and conclude with the discussion of open problems in Section VI. To encourage reproducibility and extensions to this paper, all the simulation results can be generated by the R code that is available at https://github.com/stefanwesemann/Channel-Training-Analog-FDD-Repeater

Notation and Preliminaries: Vectors and matrices are given in lowercase and uppercase boldface letters, respectively. $(\cdot)^H$ denotes the Hermitian transpose. We use the symbol E for the expectation operator. $\mathbf{1}_M$ denotes the all-ones $M \times 1$ vector, $\boldsymbol{I}_M$ denotes the $M \times M$ identity matrix. The function $\exp\{\cdot\}$ stands for the exponential, $\mathrm{etr}\{\cdot\}$ stands for the exponential of the trace of the matrix between the braces, and $\delta\cdot)$ represents the Dirac delta function. By the dominant eigenvector

©2014 IEEE. Personal use of this material is permitted. Permission from IEEE must be obtained for all other uses, in any current or future media, including reprinting/republishing this material for advertising or promotional purposes, creating new collective works, for resale or redistribution to servers or lists, or reuse of any copyrighted component of this work in other works.

S. Wesemann is with Nokia Bell Labs, Stuttgart, Germany, e-mail: stefan.wesemann@nokia-bell-labs.com.

T.L. Marzetta is with Nokia Bell Labs, Murray Hill, USA, e-mail: tom.marzetta@nokia-bell-labs.com.

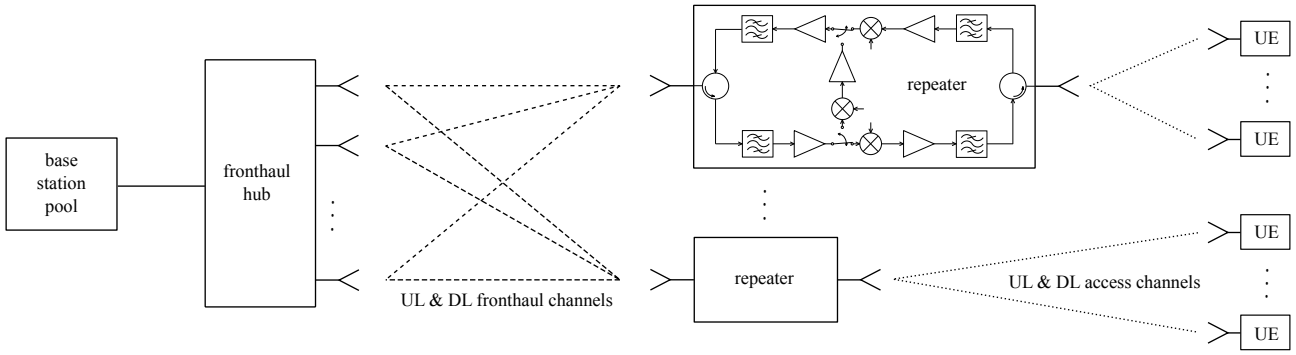

Fig. 1. An analog repeater network is shown that replaces an e.g., 4G FDD-LTE pico cell deployment. The repeaters translate the paired UL & DL carriers between the fronthaul and access bands. In the fronthaul, multiple DL (resp. UL) carriers are spatially multiplexed by the (massive) MIMO fronthaul hub. The wireless fronthaul (i.e., the cascadation of fronthaul hub, channel and repeater) is completely transparent to the base station (BS) and user equipment (UE).

$\boldsymbol{v}_{\max}(\boldsymbol{Y})$ of a matrix $\boldsymbol{Y}$, we denote the eigenvector that corresponds to the largest (i.e., dominant) eigenvalue $\lambda_{\max}(\tilde{\boldsymbol{Y}})$ of $\boldsymbol{Y}$. Two (non-zero) vectors $\boldsymbol{x}, \boldsymbol{y} \in \mathbb{C}^M$ are called equivalent $\boldsymbol{x} \sim \boldsymbol{y}$ in terms of subspaces if and only if there exists a (non-zero) scalar $a \in \mathbb{C}$ such that $\boldsymbol{x} = a \cdot \boldsymbol{y}$. This relation groups the vectors in $\mathbb{C}^M$ into equivalence classes; that is, the equivalence class of $\boldsymbol{x} \in \mathbb{C}^M$ is denoted $[\boldsymbol{x}]$, and is defined as the set $[\boldsymbol{x}] = \left\{\boldsymbol{y} \in \mathbb{C}^M | \boldsymbol{y} \sim \boldsymbol{x}\right\}$. The set of all equivalence classes forms the Grassmannian $G_1(\mathbb{C}^M)$; that is, the set of one-dimensional subspaces in $\mathbb{C}^M$. More generally, we denote the set of p-dimensional subspaces in $\mathbb{C}^M$ by $G_p(\mathbb{C}^M)$. A closely related manifold is the Stiefel manifold $V_p(\mathbb{C}^M)$, which represents the set of $M \times p$ (complex) matrices with orthonormal columns. While each point in the Stiefel manifold $V_p(\mathbb{C}^M)$ is uniquely represented by a $M \times p$ matrix, the Grassmannian $G_p(\mathbb{C}^M)$ consists of subspaces which may be specified by an arbitrary orthogonal basis stored as an $M \times p$ matrix. One should note that $V_1(\mathbb{C}^M)$ is equivalent to the $M-1$ dimensional complex hypersphere $\mathbb{S}^{M-1} \subset \mathbb{C}^M$.

II. Problem Formulation

A. System Model and Pilot Transmission

As discussed in Section I, we consider a time-invariant, frequency-flat FDD system, which consists of a fronthaul hub (FH) with M antennas and a single-antenna repeater. The UL & DL propagation channels, denoted by $\boldsymbol{g}$ and $\boldsymbol{h}$, respectively, are both modeled as $M \times 1$ complex vectors whose elements are i.i.d. $\mathcal{CN}(0, \beta)$.

In the DL, the FH antennas transmit orthogonal pilot signals of length $\tau \geq M$, which are defined by the columns of the $\tau \times M$ unitary matrix $\boldsymbol{\Phi}$, where $\boldsymbol{\Phi}^H \boldsymbol{\Phi} = \boldsymbol{I}_M$. Assuming an average transmit power per antenna of P/M, the repeater receives the weighted superposition of all pilot signals,

$$\boldsymbol{x}^H = \sqrt{\tau/MP}\boldsymbol{h}^H \boldsymbol{\Phi}^H + \boldsymbol{w}^H, \tag{1}$$

perturbed by the $\tau \times 1$ vector $\boldsymbol{w}$ which represents the receiver noise and DL interference. We model the elements of $\boldsymbol{w}$ as i.i.d. complex Gaussian noise, and take the noise variance to be 1 to minimize notation. The DL signal-to-interference-plus-noise ratio (SINR) ρ_{D}, which is defined as the ratio of the average receive power to the additive noise plus interference variance at the repeater, assuming that all FH transmit power is fed into a single antenna, is given by

$$\rho_{\mathrm{D}} = \beta P. \tag{2}$$

The repeater uses analog linear modulation [3] in order to feed back the received pilot signal to the FH. In this process, the repeater translates the DL carrier frequency to the UL carrier frequency, and scales the average power of the feedback signal by factor α. The resulting average transmit power of the repeater is denoted by $Q = \alpha(\beta P + 1)$. In the UL, the FH receives M replicas of the DL feedback signal, which are individually scaled by the components of the channel vector $\boldsymbol{g}$, and perturbed by the receiver noise and UL interference $\boldsymbol{N}$, whose elements are i.i.d. complex Gaussian with unit variance. The $M \times \tau$ receive signal is

$$\boldsymbol{Y} = \sqrt{\alpha}\boldsymbol{g}\boldsymbol{x}^H + \boldsymbol{N}. \tag{3}$$

The UL SINR ρ_{U}, which we define as the ratio of the average receive power to the additive perturbation variance at an arbitrary FH antenna, is given by

$$\rho_{\mathrm{U}} = \beta Q = \alpha\beta(\beta P + 1). \tag{4}$$

B. Pilot Reverse Modulation and Observable Invariants

Based on the received signal $\boldsymbol{Y}$, the FH has to estimate the UL & DL channels. The first processing step is the pilot reverse modulation, which consists of the right-multiplication of (3) by $\boldsymbol{\Phi}$. The resulting $M \times M$ observation matrix is

$$\begin{aligned}\tilde{\boldsymbol{Y}} &= \boldsymbol{Y}\boldsymbol{\Phi} \\ &= \sqrt{\alpha}\boldsymbol{g}\boldsymbol{x}^H\boldsymbol{\Phi} + \boldsymbol{N}\boldsymbol{\Phi} \\ &= \sqrt{\alpha\tau/MP}\boldsymbol{g}\boldsymbol{h}^H + \sqrt{\alpha}\boldsymbol{g}\tilde{\boldsymbol{w}}^H + \tilde{\boldsymbol{N}}.\end{aligned} \tag{5}$$

The elements of the transformed $M \times 1$ DL perturbation $\tilde{\boldsymbol{w}}$ and the $M \times M$ UL perturbation $\tilde{\boldsymbol{N}}$ remain i.i.d. complex Gaussian with unit variance. The pilot reverse modulation can be interpreted as a matched filtering of the received signal with the transmitted one. For the case $\tau > M$, this operation yields a noise plus interference suppression, as reflected by the post-processing UL & DL SINRs,

$$\tilde{\rho}_{\mathrm{D}} = \tau/M\beta P, \tag{6}$$

$$\tilde{\rho}_{\mathrm{U}} = \alpha\beta(\tau/M\beta P + 1). \tag{7}$$

An inspection of (5) reveals, that the UL & DL channel vectors cannot be estimated explicitly, because each vector is only observable as the outer product with an unknown vector. The only *identifiable* invariants of both, the UL & DL channels, are the subspaces $[\boldsymbol{g}]$ and $[\boldsymbol{h}]$, respectively, which are uniquely represented as elements of the Grassmannian. In addition, given the knowledge of average repeater power Q and the variance of the UL perturbations, one can estimate the (squared) norm of the UL channel vector. Note that this squared norm serves also as a reasonable estimate for DL channel vector norm because on average the DL frequency response should have approximately the same power as the UL frequency response. Thus, the only residual uncertainty in the acquired CSI is a complex phase rotation. However, it will not affect the fronthaul operations, as the internal pilots carried by the e.g., LTE signals will automatically compensate for any phase offsets.

III. Maximum Likelihood Subspace Estimation

A. Uplink Subspace Estimation and CRB

In the following, we associate elements in the Grassmannian $G_1(\mathbb{C}^M)$ with points on the hypersphere $\mathbb{S}^{M-1}$, which provides a simple problem parametrization based on Cartesian coordinates. One should note that the map between these two manifolds is not a bijection as two antipodal points on the hypersphere correspond to the same subspace. However, this ambiguity is absorbed by the likelihood function that we want to maximize in the following.

Without loss of generality, we can split the UL channel vector $\boldsymbol{g}$ into two independent random variables,

$$\boldsymbol{g} = \sqrt{\zeta}\boldsymbol{\phi}, \tag{8}$$

where $\zeta = \|\boldsymbol{g}\|^2$ is $1/2$ times a chi-square random variable with $2M$ degrees of freedom and mean value βM, and $\boldsymbol{\phi} = 1/\|\boldsymbol{g}\|\,\boldsymbol{g}$ is an isotropically distributed (i.d.) random unit vector. Their probability distribution functions (pdf) are given by

$$p(\zeta) = \frac{1}{\beta\Gamma(M)}\left(\zeta/\beta\right)^M \exp\left\{-\zeta/\beta\right\} \tag{9}$$

and

$$p(\boldsymbol{\phi}) = \frac{\Gamma(M)}{\pi^M}\delta(\boldsymbol{\phi}^H\boldsymbol{\phi} - 1). \tag{10}$$

Based on the observation matrix $\tilde{\boldsymbol{Y}}$, the ML estimate for the UL subspace (i.e., represented by a point on $\mathbb{S}^{M-1}$) is obtained as

$$\hat{\boldsymbol{g}}^{\mathrm{ML}} \sim \arg\max_{\boldsymbol{\phi}\in\mathbb{S}^{M-1}} p(\boldsymbol{\phi}|\tilde{\boldsymbol{Y}}). \tag{11}$$

Due to the isotropic distribution of $\boldsymbol{\phi}$ and the fixed probability of the given observation $\tilde{\boldsymbol{Y}}$, we have

$$\begin{aligned} p(\boldsymbol{\phi}|\tilde{\boldsymbol{Y}}) &\propto p(\tilde{\boldsymbol{Y}}, \boldsymbol{\phi}) \\ &\propto p(\tilde{\boldsymbol{Y}}|\boldsymbol{\phi}), \end{aligned} \tag{12}$$

where the latter can be written as a marginal pdf

$$p(\tilde{\boldsymbol{Y}}|\boldsymbol{\phi}) \propto \int p(\tilde{\boldsymbol{Y}}|\boldsymbol{\phi}, \zeta)p(\zeta)d\zeta. \tag{13}$$

As shown at the end of this section (Eq. (20)), the ML solution of (11) is independent of ζ. Consequently, we can set

$$p(\tilde{\boldsymbol{Y}}|\boldsymbol{\phi}) \propto p(\tilde{\boldsymbol{Y}}|\boldsymbol{\phi}, \zeta_0), \tag{14}$$

for some arbitrary but fixed ζ_0.

Since $\tilde{\boldsymbol{Y}}$ given $\boldsymbol{\phi}, \zeta_0$ is the sum of two zero-mean random Gaussian matrices, its conditional pdf is

$$\begin{aligned} p(\tilde{\boldsymbol{Y}}|\boldsymbol{\phi}, \zeta_0) = \left(\pi^M \det\boldsymbol{R}_{\tilde{\boldsymbol{Y}}|\boldsymbol{\phi},\zeta_0}\right)^{-M} \cdot \\ \operatorname{etr}\left\{-\boldsymbol{R}^{-1}_{\tilde{\boldsymbol{Y}}|\boldsymbol{\phi},\zeta_0}\tilde{\boldsymbol{Y}}\tilde{\boldsymbol{Y}}^H\right\}, \end{aligned} \tag{15}$$

where $\boldsymbol{R}_{\tilde{\boldsymbol{Y}}|\boldsymbol{\phi},\zeta_0}$ denotes the conditional covariance matrix of the columns of $\tilde{\boldsymbol{Y}}$,

$$\boldsymbol{R}_{\tilde{\boldsymbol{Y}}|\boldsymbol{\phi},\zeta_0} = \nu\boldsymbol{\phi}\boldsymbol{\phi}^H + \boldsymbol{I}_M, \tag{16}$$

with $\nu = \alpha\zeta_0(\tau/M\beta P + 1)$. The computation of its inverse and its determinant yields

$$\boldsymbol{R}^{-1}_{\tilde{\boldsymbol{Y}}|\boldsymbol{\phi},\zeta_0} = \boldsymbol{I}_M - \frac{\nu}{\nu+1}\boldsymbol{\phi}\boldsymbol{\phi}^H, \tag{17}$$

$$\det\boldsymbol{R}_{\tilde{\boldsymbol{Y}}|\boldsymbol{\phi},\zeta_0} = 1 + \nu. \tag{18}$$

Since ν is fixed, the pdf (15) reduces to

$$\begin{aligned} p(\tilde{\boldsymbol{Y}}|\boldsymbol{\phi}, \zeta_0) &\propto \exp\left\{\boldsymbol{\phi}^H\tilde{\boldsymbol{Y}}\tilde{\boldsymbol{Y}}^H\boldsymbol{\phi}\right\} \\ &\propto p(\boldsymbol{\phi}|\tilde{\boldsymbol{Y}}), \end{aligned} \tag{19}$$

which is proportional to the complex Bingham distribution [11] on $\mathbb{S}^{M-1}$, with the parameter matrix $\tilde{\boldsymbol{Y}}\tilde{\boldsymbol{Y}}^H$. For positive semi-definite parameter matrices, the function $p(\boldsymbol{\phi}|\tilde{\boldsymbol{Y}})$ has two antipodal maxima, which are achieved by the dominant eigenvector of $\tilde{\boldsymbol{Y}}\tilde{\boldsymbol{Y}}^H$, yielding the ML subspace estimate

$$\hat{\boldsymbol{g}}^{\mathrm{ML}} \sim \boldsymbol{v}_{\max}(\tilde{\boldsymbol{Y}}\tilde{\boldsymbol{Y}}^H). \tag{20}$$

One should note that this solution is independent from ζ_0, which proves the proportionality in (14).

A lower bound on subspace estimation accuracy is established by the Cramér-Rao bound (CRB), which states that the variance of any unbiased estimator is at least as high as the inverse of the Fisher information metric (FIM). Under certain regularity conditions, the FIM can be expressed using the second derivatives of the log-likelihood function $\log p([\boldsymbol{g}]|\tilde{\boldsymbol{Y}})$ with respect to the *subspace* $[\boldsymbol{g}]$. For a discussion of the difficulties that arise when computing the FIM on arbitrary manifolds in which no set of intrinsic coordinates exists, we refer the interested reader to [10]. In the following, we simply introduce the definitions that are needed for a proper interpretation of the subsequently stated CRBs.

The intrinsic version of the CRB for any unbiased estimator on the Grassmannian $G_p(\mathbb{C}^M)$ as formulated in [10], relies on the natural Riemannian metric of $G_p(\mathbb{C}^M)$. Subspace distances corresponding to this metric are given by the 2-norm of the vector of principal angles between two subspaces.

By representing one-dimensional subspaces as points on the hypersphere, the distance between $\boldsymbol{\phi}, \hat{\boldsymbol{\phi}} \in \mathbb{S}^{M-1}$ is given by

$$d_{\mathrm{ss}}(\boldsymbol{\phi}, \hat{\boldsymbol{\phi}}) = \arccos\left(|\boldsymbol{\phi}^H \hat{\boldsymbol{\phi}}|\right). \tag{21}$$

Based on this distance measure, the mean squared error (MSE) between a fixed $\boldsymbol{\phi}$ and its estimate $\hat{\boldsymbol{\phi}}$ is defined as

$$\epsilon^2_{\hat{\boldsymbol{\phi}}} = \mathrm{E}\left[d_{\mathrm{ss}}(\boldsymbol{\phi}, \hat{\boldsymbol{\phi}})^2\right], \tag{22}$$

where the expectation is with respect to the sampling distribution of $\hat{\boldsymbol{\phi}}$. For system models with the form of (3) (i.e., one-dimensional subspaces), [10] provides the inverse FIM

$$\mathcal{I}^{-1}(M, T, \gamma) = \frac{(M-1)(1+\gamma)}{T\gamma^2}, \tag{23}$$

which is parametrized by

- M : Number of FH antennas,
- T : Number of i.i.d. observation vectors (here: number of columns of $\tilde{\boldsymbol{Y}}$; i.e., $T = M$),
- γ : Effective SINR $\gamma = \zeta/\beta\tilde{\rho}_{\mathrm{U}}$, assuming a unit norm channel vector.

This inverse FIM provides the CRB on the natural subspace distance between the true subspace and any unbiased estimate of it. For a *fixed* realization $\boldsymbol{g}$, we have the uplink CRB

$$\epsilon^2_{\hat{\boldsymbol{g}}} \geq \mathcal{I}^{-1}(M, M, \zeta/\beta\tilde{\rho}_{\mathrm{U}}) \quad (\mathrm{rad}^2). \tag{24}$$

In order to obtain an average CRB for random $\boldsymbol{g}$, we have to take the expectation with respect to ζ. By the Jensen's inequality and the convexity of $\mathcal{I}^{-1}(M, T, \gamma)$ with respect to γ, we obtain the inequality

$$\begin{aligned}\bar{\epsilon}^2_{\hat{\boldsymbol{g}}} = \mathrm{E}\left[\epsilon^2_{\hat{\boldsymbol{g}}}\right] &\geq \mathrm{E}\left[\mathcal{I}^{-1}(M, M, \zeta/\beta\tilde{\rho}_{\mathrm{U}})\right] \\ &\geq \mathcal{I}^{-1}(M, M, \mathrm{E}[\zeta]/\beta\tilde{\rho}_{\mathrm{U}}) \\ &= \mathcal{I}^{-1}(M, M, M\tilde{\rho}_{\mathrm{U}}) \quad (\mathrm{rad}^2).\end{aligned} \tag{25}$$

Remark 1. One should note that the CRB (24) relies on a truncated Taylor expansion. For the differentiation of the first derivatives on the Grassmannian, an additional structure (i.e., affine connection) has been introduced, which allows to connect tangent spaces at different points of the manifold. In [10], the sectional and Riemannian curvature terms that appear in the CRB because of the affine connection have been omitted for the sake of closed-form expressions. As we will illustrate in Section V, the resulting CRB is legitimate only at a large enough SINR so that typical errors are small compared to the scale at which curvature becomes a dominant feature.

B. Downlink Subspace Estimation and CRB

For the estimation of the DL subspace, we consider the conjugate transposed of the system model in (5),

$$\tilde{\boldsymbol{Y}}^H = \sqrt{\alpha}\underbrace{\left[\sqrt{\tau P/M}\boldsymbol{h} + \tilde{\boldsymbol{w}}\right]}_{\tilde{\boldsymbol{x}}}\boldsymbol{g}^H + \tilde{\boldsymbol{N}}^H, \tag{26}$$

where $\boldsymbol{h}$ is fixed but unknown, and $\boldsymbol{g}$ is a complex Gaussian random vector. Analog to the previous section, we associate subspaces with points on the hypersphere, and exploit the independence of ML estimator for $[\boldsymbol{h}]$ with respect to the norm of $\boldsymbol{h}$. Consequently, the ML estimate for the DL subspace, given the observation $\tilde{\boldsymbol{Y}}$, is obtained by

$$\hat{\boldsymbol{h}}^{\mathrm{ML}} \sim \arg\max_{\boldsymbol{h}\in\mathbb{S}^{M-1}} p(\boldsymbol{h}|\tilde{\boldsymbol{Y}}), \tag{27}$$

where $p(\boldsymbol{h}|\tilde{\boldsymbol{Y}})$ denotes the conditional pdf of $\boldsymbol{h}$ given $\tilde{\boldsymbol{Y}}$. Due to the existence of the term $\tilde{\boldsymbol{w}}\boldsymbol{g}^H$ in (26), which follows a (degenerate) complex double Gaussian distribution [12], no closed-form expression for $p(\boldsymbol{h}|\tilde{\boldsymbol{Y}})$ is available. However, by introducing the auxiliary variable $\tilde{\boldsymbol{x}}$, (26) forms the Markov chain

$$\boldsymbol{h} \overset{p(\tilde{\boldsymbol{x}}|\boldsymbol{h})}{\longrightarrow} \tilde{\boldsymbol{x}} \overset{p(\tilde{\boldsymbol{Y}}|\tilde{\boldsymbol{x}})}{\longrightarrow} \tilde{\boldsymbol{Y}}, \tag{28}$$

whose joint pdf is

$$p(\boldsymbol{h}, \tilde{\boldsymbol{x}}, \tilde{\boldsymbol{Y}}) = p(\boldsymbol{h})p(\tilde{\boldsymbol{x}}|\boldsymbol{h})p(\tilde{\boldsymbol{Y}}|\tilde{\boldsymbol{x}}). \tag{29}$$

Consequently, the conditional pdf $p(\boldsymbol{h}|\tilde{\boldsymbol{Y}})$ can be written as the marginal distribution

$$\begin{aligned}p(\boldsymbol{h}|\tilde{\boldsymbol{Y}}) &= \int p(\boldsymbol{h}, \tilde{\boldsymbol{x}}|\tilde{\boldsymbol{Y}})\, d\tilde{\boldsymbol{x}} \\ &\propto \int p(\boldsymbol{h}, \tilde{\boldsymbol{x}}, \tilde{\boldsymbol{Y}})\, d\tilde{\boldsymbol{x}} \\ &\propto \int p(\tilde{\boldsymbol{x}}|\boldsymbol{h})p(\tilde{\boldsymbol{Y}}|\tilde{\boldsymbol{x}})\, d\tilde{\boldsymbol{x}} \\ &\propto \int p(\boldsymbol{h}|\tilde{\boldsymbol{x}})p(\tilde{\boldsymbol{x}}|\tilde{\boldsymbol{Y}})\, d\tilde{\boldsymbol{x}},\end{aligned} \tag{30}$$

where we exploited the fact that $\boldsymbol{h}$ and $\tilde{\boldsymbol{x}}$ are isotropically distributed, and the irrelevance of the fixed probability $p(\tilde{\boldsymbol{Y}})$ with respect to our inference problem.

The ML estimate for the subspace of $\boldsymbol{h}$ is thus obtained by

$$\hat{\boldsymbol{h}}^{\mathrm{ML}} \sim \arg\max_{\boldsymbol{h}\in\mathbb{S}^{M-1}} \int p(\boldsymbol{h}|\tilde{\boldsymbol{x}})p(\tilde{\boldsymbol{x}}|\tilde{\boldsymbol{Y}})\, d\tilde{\boldsymbol{x}}, \tag{31}$$

where the conditional pdf $p(\boldsymbol{h}|\tilde{\boldsymbol{x}})$ is

$$\begin{aligned}p(\boldsymbol{h}|\tilde{\boldsymbol{x}}) &\propto p(\tilde{\boldsymbol{x}}|\boldsymbol{h}) \\ &= \left(\pi^M \det\boldsymbol{R}_{\tilde{\boldsymbol{x}}|\boldsymbol{h}}\right)^{-1} \exp\left\{-\tilde{\boldsymbol{x}}^H \boldsymbol{R}^{-1}_{\tilde{\boldsymbol{x}}|\boldsymbol{h}}\tilde{\boldsymbol{x}}\right\},\end{aligned} \tag{32}$$

with

$$\boldsymbol{R}_{\tilde{\boldsymbol{x}}|\boldsymbol{h}} = \mathrm{E}\left[\tilde{\boldsymbol{x}}\tilde{\boldsymbol{x}}^H|\boldsymbol{h}\right] = \tau/MP\boldsymbol{h}\boldsymbol{h}^H + \boldsymbol{I}_M. \tag{33}$$

Because of $\boldsymbol{h} \in \mathbb{S}^{M-1}$, the conditional probability $p(\boldsymbol{h}|\tilde{\boldsymbol{x}})$ is again (cf. Section III-A) proportional to the complex Bingham distribution with the parameter matrix $\tilde{\boldsymbol{x}}\tilde{\boldsymbol{x}}^H$, whose maximum is attained by choosing $\boldsymbol{h} \sim \tilde{\boldsymbol{x}}$. Consequently, the function $p(\boldsymbol{h}|\tilde{\boldsymbol{x}})$ can be replaced by $\delta(\boldsymbol{h} - \tilde{\boldsymbol{x}})$ without changing the maximizing argument in (31); that is,

$$\begin{aligned}\hat{\boldsymbol{h}}^{\mathrm{ML}} &\sim \arg\max_{\boldsymbol{h}\in\mathbb{S}^{M-1}} \int \delta(\boldsymbol{h} - \tilde{\boldsymbol{x}})p(\tilde{\boldsymbol{x}}|\tilde{\boldsymbol{Y}})d\tilde{\boldsymbol{x}} \\ &\sim \arg\max_{\tilde{\boldsymbol{x}}\in\mathbb{S}^{M-1}} p(\tilde{\boldsymbol{x}}|\tilde{\boldsymbol{Y}}),\end{aligned} \tag{34}$$

where the last step exploits $\tilde{\boldsymbol{x}} \sim \boldsymbol{h}$. Finally, we need to find the subspace that maximizes $p(\tilde{\boldsymbol{x}}|\tilde{\boldsymbol{Y}})$. Analog to Section III-A, $\tilde{\boldsymbol{Y}}$ given $\tilde{\boldsymbol{x}}$ is zero-mean and Gaussian, and its conditional pdf $p(\tilde{\boldsymbol{Y}}|\tilde{\boldsymbol{x}}) \propto p(\tilde{\boldsymbol{x}}|\tilde{\boldsymbol{Y}})$ is given by

$$p(\tilde{\boldsymbol{Y}}|\tilde{\boldsymbol{x}}) = \left(\pi^M \det\boldsymbol{R}_{\tilde{\boldsymbol{Y}}|\tilde{\boldsymbol{x}}}\right)^{-M} \mathrm{etr}\left\{-\boldsymbol{R}^{-1}_{\tilde{\boldsymbol{Y}}|\tilde{\boldsymbol{x}}}\tilde{\boldsymbol{Y}}^H\tilde{\boldsymbol{Y}}\right\}, \tag{35}$$

where $\boldsymbol{R}_{\tilde{\boldsymbol{Y}}|\tilde{\boldsymbol{x}}}$ denotes the conditional covariance matrix for the rows of $\tilde{\boldsymbol{Y}}$,

$$\boldsymbol{R}_{\tilde{\boldsymbol{Y}}|\tilde{\boldsymbol{x}}} = \alpha\beta\tilde{\boldsymbol{x}}\tilde{\boldsymbol{x}}^H + \boldsymbol{I}_M. \tag{36}$$

Since we can again assume $\tilde{\boldsymbol{x}} \in \mathbb{S}^{M-1}$, the computation of the determinant and the inverse of $\boldsymbol{R}_{\tilde{\boldsymbol{Y}}|\tilde{\boldsymbol{x}}}$ shows that $p(\tilde{\boldsymbol{Y}}|\tilde{\boldsymbol{x}})$ is proportional to the Bingham distribution with the parameter matrix $\tilde{\boldsymbol{Y}}^H\tilde{\boldsymbol{Y}}$; that is,

$$p(\tilde{\boldsymbol{x}}|\tilde{\boldsymbol{Y}}) \propto p(\tilde{\boldsymbol{Y}}|\tilde{\boldsymbol{x}}) \propto \exp\left\{\tilde{\boldsymbol{x}}^H\tilde{\boldsymbol{Y}}^H\tilde{\boldsymbol{Y}}\tilde{\boldsymbol{x}}\right\}. \tag{37}$$

The maximizing argument $\tilde{\boldsymbol{x}} \sim \hat{\boldsymbol{h}}^{\mathrm{ML}}$ is given by the dominant eigenvector of $\tilde{\boldsymbol{Y}}^H\tilde{\boldsymbol{Y}}$,

$$\hat{\boldsymbol{h}}^{\mathrm{ML}} \sim \boldsymbol{v}_{\max}(\tilde{\boldsymbol{Y}}^H\tilde{\boldsymbol{Y}}). \tag{38}$$

The CRB for the DL subspace estimator consists of two components. First note that the (transformed) DL perturbations $\tilde{\boldsymbol{w}}$ constitute a residual impairment because the ML subspace estimate $[\hat{\boldsymbol{h}}^{\mathrm{ML}}]$ equals $[\tilde{\boldsymbol{x}}]$. The MSE caused by this residual perturbation is lower bound by the CRB $\bar{\epsilon}^2_{\boldsymbol{h},\mathrm{D}}$ of the estimator for $[\boldsymbol{h}]$ given the single (DL) observation $\tilde{\boldsymbol{x}}$. Again, we can apply the inverse FIM (23) with $T = 1$, and the (average) effective SINR $\bar{\gamma}_{\boldsymbol{h},\mathrm{D}} = \mathrm{E}\left[\|\boldsymbol{h}\|^2\right]/\beta\tilde{\rho}_{\mathrm{D}} = M\tilde{\rho}_{\mathrm{D}}$, yielding the first CRB component

$$\bar{\epsilon}^2_{\boldsymbol{h},\mathrm{D}} \geq \mathcal{I}^{-1}(M, 1, M\tilde{\rho}_{\mathrm{D}}) \quad (\mathrm{rad}^2). \tag{39}$$

The second subspace error component is due to the UL perturbation, which limits the estimation accuracy when estimating $\boldsymbol{h} \sim \tilde{\boldsymbol{x}}$ from the UL observation $\tilde{\boldsymbol{Y}}$. Employing the inverse FIM (23) with $T = M$, and the (average) effective SINR $M\tilde{\rho}_{\mathrm{U}}$ (cf. Section III-A), we have the second CRB component

$$\bar{\epsilon}^2_{\boldsymbol{h},\mathrm{U}} \geq \mathcal{I}^{-1}(M, M, M\tilde{\rho}_{\mathrm{U}}) \quad (\mathrm{rad}^2). \tag{40}$$

Due to the independence of the UL & DL perturbations, the resulting total CRB is given by the sum of the individual error variances; that is,

$$\bar{\epsilon}^2_{\boldsymbol{h}} \geq \mathcal{I}^{-1}(M, 1, M\tilde{\rho}_{\mathrm{D}}) + \mathcal{I}^{-1}(M, M, M\tilde{\rho}_{\mathrm{U}}). \tag{41}$$

Remark 2. A comparison of (25) with (41) shows, that for finite $\tilde{\rho}_{\mathrm{D}}$ the accuracy of the UL subspace estimator always excels the accuracy of the DL estimator. There is no way to change this behavior by means of power control at the FH and/or repeater.

C. Reduction of the Computational Complexity

For the joint estimation of the UL & DL subspaces, we need to compute the dominant eigenvectors $\boldsymbol{v}_{\max}(\tilde{\boldsymbol{Y}}\tilde{\boldsymbol{Y}}^H)$ and $\boldsymbol{v}_{\max}(\tilde{\boldsymbol{Y}}^H\tilde{\boldsymbol{Y}})$. Both can be simultaneously obtained with the SVD

$$\tilde{\boldsymbol{Y}} := \boldsymbol{U}\boldsymbol{\Sigma}\boldsymbol{V}^H. \tag{42}$$

The columns of $\boldsymbol{U} = [\boldsymbol{u}_1, \ldots, \boldsymbol{u}_M]$ and $\boldsymbol{V} = [\boldsymbol{v}_1, \ldots, \boldsymbol{v}_M]$ denote the left- and right-singular vectors of $\tilde{\boldsymbol{Y}}$, and $\boldsymbol{\Sigma}$ is the diagonal matrix (sorted in descending order) of singular values $\{\sigma_m\}_{m=1}^M$. The ML estimates for UL & DL subspaces are given by left- and right-singular vectors that correspond to the largest singular value σ_1; that is,

$$\hat{\boldsymbol{g}}^{\mathrm{ML}} \sim \boldsymbol{u}_1, \tag{43}$$

$$\hat{\boldsymbol{h}}^{\mathrm{ML}} \sim \boldsymbol{v}_1. \tag{44}$$

1) SVD via Power Iterations: The computational (time) complexity of the SVD algorithm for a square $M \times M$ matrix $\tilde{\boldsymbol{Y}}$ is generally $\mathcal{O}(M^3)$; that is, it is not well-suited for high-dimensional matrices. However, the dominant left- and right-singular vectors of $\tilde{\boldsymbol{Y}}$ that correspond to the largest singular value, can be easily approximated by using the power iteration method [13, Section 7.3.1]. For example, the UL subspace estimate $\hat{\boldsymbol{g}}^{\mathrm{ML}}$ is iteratively approximated by the recurrence relation

$$\hat{\boldsymbol{g}}_i = \tilde{\boldsymbol{Y}}\tilde{\boldsymbol{Y}}^H\hat{\boldsymbol{g}}_{i-1}/\|\tilde{\boldsymbol{Y}}\tilde{\boldsymbol{Y}}^H\hat{\boldsymbol{g}}_{i-1}\|. \tag{45}$$

If we assume that the matrix $\tilde{\boldsymbol{Y}}\tilde{\boldsymbol{Y}}^H$ has an eigenvalue that is strictly greater in magnitude than its other eigenvalues, and the starting vector $\hat{\boldsymbol{g}}_0$ has a nonzero dot product with the dominant eigenvector of $\tilde{\boldsymbol{Y}}\tilde{\boldsymbol{Y}}^H$, then a subsequence $(\hat{\boldsymbol{g}}_i)$ converges to the true dominant eigenvector. As a simple stopping criterion, we propose using the distance $d_{\mathrm{ss}}(\hat{\boldsymbol{g}}_i, \hat{\boldsymbol{g}}_{i-1})$ between two consecutively computed subspaces, which is required to be smaller than a predefined threshold δ. For a given $\hat{\boldsymbol{g}}_i$, the corresponding left-singular vector $\hat{\boldsymbol{h}}^{\mathrm{ML}}$ and the singular value $\hat{\sigma}_1$ are calculated by

$$\hat{\boldsymbol{h}} = \tilde{\boldsymbol{Y}}^H\hat{\boldsymbol{g}}_i/\|\tilde{\boldsymbol{Y}}^H\hat{\boldsymbol{g}}_i\| \tag{46}$$

$$\hat{\sigma}_1 = |\hat{\boldsymbol{g}}^H\tilde{\boldsymbol{Y}}\hat{\boldsymbol{h}}_i|. \tag{47}$$

If the number of required power iterations is smaller than $\frac{M^2}{M+1} + 1$, then the joint complexity (in terms of dot products) of the computations (45), (46) can be reduced by splitting the matrix-vector product in (45) (which requires a non-recurring matrix-matrix multiplication) into two successive steps,

$$\hat{\boldsymbol{h}}_i = \tilde{\boldsymbol{Y}}^H\hat{\boldsymbol{g}}_{i-1}/\|\tilde{\boldsymbol{Y}}^H\hat{\boldsymbol{g}}_{i-1}\| \tag{48}$$

$$\hat{\boldsymbol{g}}_i = \tilde{\boldsymbol{Y}}\hat{\boldsymbol{h}}_i/\|\tilde{\boldsymbol{Y}}\hat{\boldsymbol{h}}_i\|. \tag{49}$$

One should note that the number of required iterations strongly depends on the initial value $\hat{\boldsymbol{g}}_0$. Therefore, we propose using the column of $\tilde{\boldsymbol{Y}} = [\tilde{\boldsymbol{y}}_1, \ldots, \tilde{\boldsymbol{y}}_M]$ with the largest Euclidean norm because it has the smallest (relative) noise perturbation with a high probability. The overall procedure is summarized in Algorithm 1, where we extended the stopping criterion by the DL subspace increment.

2) Shifting/Omitting the Pilot Reverse Modulation: For the UL subspace estimation with $\tau/M = 1$, the pilot reverse modulation step in (5) can be omitted because the left-singular vectors $\boldsymbol{U} = [\boldsymbol{u}_1, \ldots, \boldsymbol{u}_M]$ of $\tilde{\boldsymbol{Y}} := \boldsymbol{U}\boldsymbol{\Sigma}\boldsymbol{V}^H$ and $\boldsymbol{Y} := \boldsymbol{U}\boldsymbol{\Sigma}\tilde{\boldsymbol{V}}^H = \boldsymbol{U}\boldsymbol{\Sigma}\boldsymbol{V}^H\boldsymbol{\Phi}^H$ span the same subspaces.

Similarly for the DL subspace estimation with $\tau/M = 1$, the order of the pilot reverse modulation step and the SVD-based DL subspace estimation can be swapped; that is,

$$\hat{\boldsymbol{h}} \sim \boldsymbol{\Phi}^H\tilde{\boldsymbol{v}}_1. \tag{50}$$

where $\tilde{\boldsymbol{v}}_1$ denotes the right-singular vector of $\boldsymbol{Y} := \boldsymbol{U}\boldsymbol{\Sigma}\left[\tilde{\boldsymbol{v}}_1, \ldots, \tilde{\boldsymbol{v}}_M\right]^H$. Note that we have $\tilde{\boldsymbol{v}}_1 = \boldsymbol{\Phi}\boldsymbol{v}_1$ with $\boldsymbol{v}_1$

Algorithm 1 Rank-1 SVD based on Power Iterations

procedure POWERITERATION($\tilde{\boldsymbol{Y}}, \delta$)
  $m^* \leftarrow \arg\max_{m\in[1,M]} \|\tilde{\boldsymbol{y}}_m\|^2$
  $\hat{\boldsymbol{g}}_0 \leftarrow \tilde{\boldsymbol{y}}_{m^*}/\|\tilde{\boldsymbol{y}}_{m^*}\|$
  $\hat{\boldsymbol{h}}_0 \leftarrow M^{-\frac{1}{2}}\mathbf{1}_M$
  $i \leftarrow 0$
  repeat
    $i \leftarrow i+1$
    $\hat{\boldsymbol{h}}_i \leftarrow \tilde{\boldsymbol{Y}}^H\hat{\boldsymbol{g}}_{i-1}/\|\tilde{\boldsymbol{Y}}^H\hat{\boldsymbol{g}}_{i-1}\|$
    $\hat{\boldsymbol{g}}_i \leftarrow \tilde{\boldsymbol{Y}}\hat{\boldsymbol{h}}_i/\|\tilde{\boldsymbol{Y}}\hat{\boldsymbol{h}}_i\|$
  until $(\max\{d_{\text{ss}}(\hat{\boldsymbol{g}}_{i-1},\hat{\boldsymbol{g}}_i), d_{\text{ss}}(\hat{\boldsymbol{h}}_{i-1},\hat{\boldsymbol{h}}_i)\} \le \delta)$
  $\hat{\sigma}_1 \leftarrow |\hat{\boldsymbol{g}}_i^H\tilde{\boldsymbol{Y}}\hat{\boldsymbol{h}}_i|$
  return $\hat{\boldsymbol{h}}_i, \hat{\boldsymbol{g}}_i, \hat{\sigma}_1$
end procedure

given in (42). Consequently, the matrix-matrix multiplication in (5) can be reduced to a matrix-vector multiplication, which incurs no performance loss for the case $\tau/M = 1$.

IV. Uplink Channel Gain Estimation

For a proper power control of the fronthaul links, knowledge of the UL & DL channel gains is required. Ideally, these gains are estimated separately, but an inspection of the feedback signal in (5) reveals that without any knowledge of the DL perturbation variance, the FH cannot derive an estimate for the DL channel vector norm. Since we assume fully analog repeaters, there exists no simply way to estimate and feedback DL perturbation variance to the FH. Consequently, we focus on the estimation of the UL channel vector norm, and exploit the fact that on average the DL frequency response has approximately the same power as the UL frequency response, so that it is reasonable to assume them to be equal.

A. Maximum Likelihood Estimation

Again, we split the UL channel vector into two independent random variables (cf. (8)). The reverse-modulated UL signal (5) becomes

$$\tilde{\boldsymbol{Y}} = \sqrt{\alpha\zeta}\boldsymbol{\phi}\tilde{\boldsymbol{x}}^H + \tilde{\boldsymbol{N}} \tag{51}$$

where $\tilde{\boldsymbol{x}} = \boldsymbol{\Phi}^H\boldsymbol{x}$. In the following, we are interested in the ML estimate for ζ, in presence of the unknown

- isotropically distributed complex unit vector $\boldsymbol{\phi} \in \mathbb{S}^{M-1}$,
- complex Gaussian signal $\sqrt{\alpha}\tilde{\boldsymbol{x}} \in \mathbb{C}^M$ with i.i.d. entries of variance $\tilde{Q} = \alpha(\tau/M\beta P + 1)$,
- complex Gaussian perturbation $\tilde{\boldsymbol{N}} \in \mathbb{C}^{M\times M}$ with i.i.d. entries of unit variance.

We assume that the FH knows the (effective) transmit power $\tilde{Q}$ of the repeater, and the variance of the UL perturbations.

The ML estimate for ζ is defined as

$$\hat{\zeta}^{\text{ML}} = \arg\max_{\zeta\in\mathbb{R}_+} p(\zeta|\tilde{\boldsymbol{Y}}). \tag{52}$$

Due to the uniform distribution of ζ on $\mathbb{R}_+$ and the fixed probability of the given observation $\tilde{\boldsymbol{Y}}$, we have

$$p(\zeta|\tilde{\boldsymbol{Y}}) \propto p(\tilde{\boldsymbol{Y}}|\zeta). \tag{53}$$

The conditional pdf $p(\tilde{\boldsymbol{Y}}|\zeta)$ can be written as the marginal pdf,

$$p(\tilde{\boldsymbol{Y}}|\zeta) = \int p(\tilde{\boldsymbol{Y}}|\boldsymbol{\phi},\zeta)p(\boldsymbol{\phi})d\boldsymbol{\phi}, \tag{54}$$

where $p(\tilde{\boldsymbol{Y}}|\boldsymbol{\phi},\zeta)$ and $p(\boldsymbol{\phi})$ are given by (15) and (10), repsectively. With $q(\zeta) = \zeta\tilde{Q}/(1+\zeta\tilde{Q})$, the pdf in (54) becomes

$$\begin{aligned} p(\tilde{\boldsymbol{Y}}|\zeta) \propto& \frac{1}{(1+\zeta\tilde{Q})^M}\int \text{etr}\left\{q(\zeta)\boldsymbol{\phi}^H\tilde{\boldsymbol{Y}}\tilde{\boldsymbol{Y}}^H\boldsymbol{\phi}\right\}p(\boldsymbol{\phi})d\boldsymbol{\phi} \\ =& \frac{1}{(1+\zeta\tilde{Q})^M}\int \text{etr}\left\{q(\zeta)\boldsymbol{\phi}^H\boldsymbol{U}\boldsymbol{\Sigma}^2\boldsymbol{U}^H\boldsymbol{\phi}\right\}p(\boldsymbol{\phi})d\boldsymbol{\phi} \\ =& \frac{1}{(1+\zeta\tilde{Q})^M}\int \text{etr}\left\{q(\zeta)\sum_{m=1}^M |\phi_m|^2\sigma_m^2\right\}p(\boldsymbol{\phi})d\boldsymbol{\phi} \end{aligned} \tag{55}$$

where we use the eigendecomposition $\tilde{\boldsymbol{Y}}\tilde{\boldsymbol{Y}}^H = \boldsymbol{U}\boldsymbol{\Sigma}^2\boldsymbol{U}^H$ (cf. (42)), and $\{\sigma_m^2\}_{m=1}^M$ denote the diagonal elements of $\boldsymbol{\Sigma}^2$. In the above, we change the integration variable from $\boldsymbol{\phi}$ to $\boldsymbol{U}^H\boldsymbol{\phi}$, and use the fact that $\boldsymbol{U}^H\boldsymbol{\phi}$ has the same probability density as $\boldsymbol{\phi}$. Since we have almost surely $\sigma_1^2 > \sigma_2^2 > \ldots > \sigma_M^2 > 0$, a closed-form expression [14, Section B.1] for (55) is given by

$$p(\tilde{\boldsymbol{Y}}|\zeta) \propto \frac{1}{(1+\zeta\tilde{Q})^M}\sum_{m=1}^M \frac{e^{q(\zeta)\sigma_m^2} - e^{q(\zeta)\sigma_1^2}}{\prod_{n\neq m} q(\zeta)(\sigma_m^2-\sigma_n^2)}. \tag{56}$$

Apparently, there is no closed-form expression for the argument $\hat{\zeta}^{\text{ML}}$ that maximizes (56). By the problem structure, however, (56) has a unique maximum, which can be found e.g., by the Golden section method [15, Appendix C.3].

B. SCM-based Estimation

The structure of the covariance matrix $\boldsymbol{R}_{\tilde{\boldsymbol{Y}}|\boldsymbol{g}}$ in (16) reveals an alternative approach for the UL channel norm estimation. Its eigenvalues are given by $\left\{\zeta\tilde{Q}+1, 1, \ldots, 1\right\}$. So, by computing the sample covariance matrix (SCM)

$$\hat{\boldsymbol{R}}_{\tilde{\boldsymbol{Y}}|\boldsymbol{g}} = M^{-1}\tilde{\boldsymbol{Y}}\tilde{\boldsymbol{Y}}^H, \tag{57}$$

an estimate for ζ can be derived from its largest eigenvalue $\lambda_{\max}(\hat{\boldsymbol{R}}_{\tilde{\boldsymbol{Y}}|\boldsymbol{g}})$; that is,

$$\hat{\zeta} = \frac{\lambda_{\max}(\hat{\boldsymbol{R}}_{\tilde{\boldsymbol{Y}}|\boldsymbol{g}}) - 1}{\tilde{Q}} = \frac{\sigma_1^2 - M}{\tilde{Q}M} \tag{58}$$

where σ_1 denotes the largest singular value in (42). The accuracy of this estimate strongly depends on the accuracy of the SCM, which is only asymptotically efficient (i.e., for large values of M). For low sample support, the SCM is biased and not efficient with respect to the natural covariance metric [10, Section III.C].

Remark 3. The same estimator is obtained by

$$\hat{\zeta} = \arg\max_{\zeta\in\mathbb{R}_+} p(\tilde{\boldsymbol{Y}}|\boldsymbol{\phi} = \hat{\boldsymbol{g}}^{\text{ML}}, \zeta) \tag{59}$$

$$= \arg\max_{\zeta\in\mathbb{R}_+} \frac{1}{(1+\zeta\tilde{Q})^M}e^{q(\zeta)\sigma_1^2} \tag{60}$$

$$= \frac{\sigma_1^2 - M}{\tilde{Q}M}$$

where $p(\tilde{\boldsymbol{Y}}|\boldsymbol{\phi},\zeta)$ is given in (15), and $\hat{\boldsymbol{g}}^{\mathrm{ML}}$ is the ML estimate for the UL subspace given in (20).

V. Numerical Illustration

Our analytical results in Section III are corroborated by Monte Carlo simulations, which compare the subspace estimation accuracies of SVD-based estimator and the power iteration method against the CRBs. In our simulations, we set $\tau = M$ and assume genie power control at the repeater side. Therefore, the repeater exploits perfect knowledge of the UL perturbation variance β_{U} in order to adjust its scaling factor

$$\alpha = \frac{\rho_{\mathrm{U}}}{\beta(\beta P + 1}, \tag{61}$$

such that a predefined UL SINR ρ_{U} is achieved.

Given a parameter set $\{M, \rho_{\mathrm{D}}, \rho_{\mathrm{U}}\}$, the CRBs are computed according to (25) and (41), and 1000 Monte Carlo trials are performed. For each trial, the unitary pilot matrix $\boldsymbol{\Phi}$ is chosen randomly from the uniform distribution on the Stiefel manifold $V_M(\mathbb{C}^\tau)$, whereas the UL & DL channel vectors and perturbations are generated according to Section II.

The left side of Figure 2 shows the achieved UL root mean square error (RMSE), which is independent of ρ_{D} because of $\tau = M$, and right side shows the DL RMSEs (for a fixed $\rho_{\mathrm{U}} =$ 10dB) as a function of the UL and DL SINRs, respectively. As already noted in [10], the SVD-based estimator (green curve) is unbiased and asymptotically efficient; that is, its accuracy approaches asymptotically the CRB (red curve) as the number of observations $M(=\tau)$ becomes large. On the other hand, the CRB fails as a lower bound for low SINRs because it does not incorporate the sectional and Riemannian curvature terms as argued in [16, Section IV]. Neglecting these terms can be legitimized for small errors only. For our system model, the CRB's range of validity is lower bounded by $\rho_{\mathrm{U}} > 0$dB and $\rho_{\mathrm{D}} > 10\mathrm{lg}(M)$dB. In addition, the blue curves in Figure 2 display the subspace RMSE for the power iteration based estimator, using the stopping criterion $\delta = 10^{-1}$. Over typical ranges of the SINR parameters, the performance difference with respect to the SVD-based method is negligible.

In order to assess the computational complexity of the power iteration method, Figure 4 shows the average number of power iterations as a function of M, for various parameter combinations of ρ_{U} and δ. In each subplot, we depict the shape the iteration number's cumulative distribution function (CDF) by a shaded area, which is lower and upper bounded by the 5th- and 95th-percentile of the CDF, respectively. The solid blue curve depicts the average number of iterations. We see that the number of required iterations decreases for increasing M and ρ_{U}; that is, the number of iterations can be upper bounded, which yields a quadratic time complexity with respect to M. One should note that for low SINRs, the distance between the largest and second-largest eigenvalue of $\tilde{\boldsymbol{Y}}\tilde{\boldsymbol{Y}}^H$ decreases, which results in a slower convergence.

Finally, we analyze the relative bias and error variance for the UL channel gain estimators described in Section IV, assuming $Q = 1$ which yields $\beta = \rho_{\mathrm{U}}$. Due to the exponential terms in (56), the ML estimator is numerically intractable for large M and β. Therefore, we omit all data points that

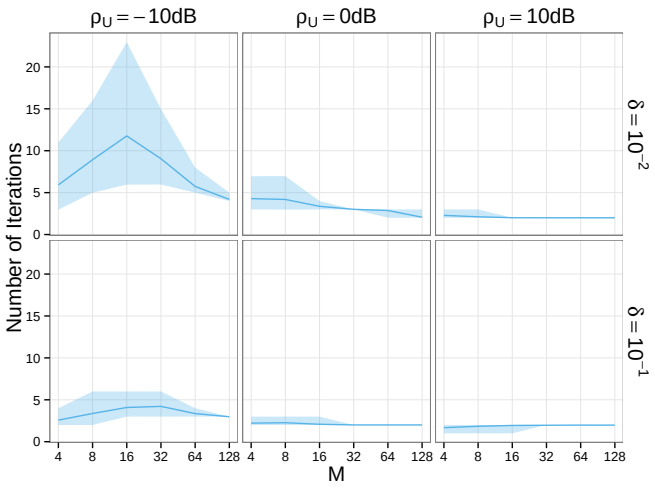

Fig. 4. Number of power iterations as a function of the number of FH antennas M, for different UL SINRs ρ_{U} and accuracy bounds δ. The solid line depicts the average number of iterations. The shade area illustrates the 5th- and 95th-percentiles of the iteration number's CDF. For low UL SINRs, the number required iterations grows because the distance between largest and second largest eigenvalues of decreases.

exhibit numerical overflows. The left side of Figure 3 shows the relative bias of the estimators. For a sufficient number (i.e., $M \geq 8$) of UL observations, the ML estimator (52) is unbiased for all simulated values of $\beta = \rho_{\mathrm{U}}$. This is quite remarkable because for $\rho_{\mathrm{U}} = -10$dB the signal component in the observation is 10 times weaker than the perturbations. In contrast, the SCM-based estimator exhibits a significant bias for small ρ_{U}, which of course decreases as the number of available observations M grows. Regarding the relative error variance as shown on the right side of Figure 3, both estimators exhibit a similar performance, which improves with growing M because of the number of UL observations increases.

VI. Summary and Discussion

For the UL subspace estimation, we have shown that the subspace which maximizes the likelihood function is given by the dominant eigenvector of the sample covariance matrix for the FH's observations. For the DL subspace, no closed-form expression for the likelihood function exists due to the presence of a degenerate double Gaussian term. However, by exploiting the Markovian property of the signal model, we could show that the problem of finding the maximum likelihood estimate reduces to the maximization of the likelihood function for the received signal at the repeater. The solution is given by the dominant eigenvector of the sample covariance matrix for the conjugate transposed of the FH's observation matrix. Consequently, both estimates can be obtained simultaneously by computing the SVD of the pilot-reverse modulated receive signal. This result is all the more intuitive because we assumed spatially and temporally white perturbations, and also because the SVD is the optimal estimator for the noise-free case.

Based on the inverse Fisher information metric (FIM) from [10], we have formulated the CRBs for the unbiased UL

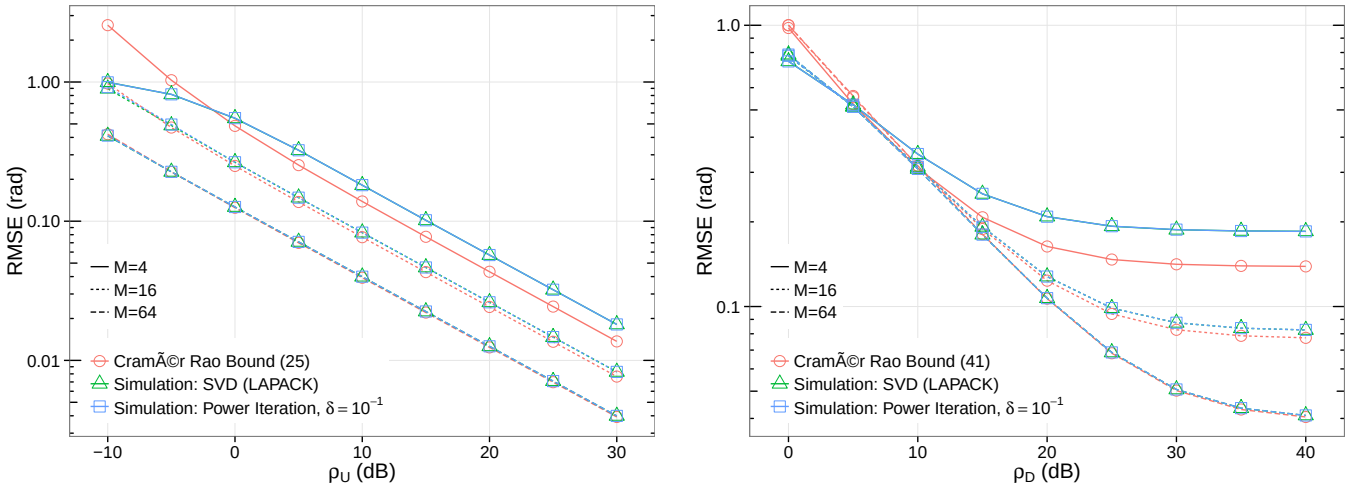

Fig. 2. Comparison between the {SVD, Power Iteration}-based subspace estimator's RMSE and the CRB for $M = \{4, 16, 64\}, \tau = M$; a) in the left figure as a function of the UL SINR ρ_{U}, b) in the right figure as a function of the DL SINR ρ_{D} with fixed $\rho_{\mathrm{U}} = 10$dB. Observe that the accuracy of the SVD-based estimator asymptotically approaches the CRB as $M(= \tau) \to \infty$; that is, the estimator is unbiased and asymptotically efficient. Moreover, one should note that the CRB fails for low SINRs (i.e., $\rho_{\mathrm{U}} < 0$dB, $\rho_{\mathrm{D}} < 10\mathrm{lg}(M)$dB) because it relies on truncated Taylor expansions.

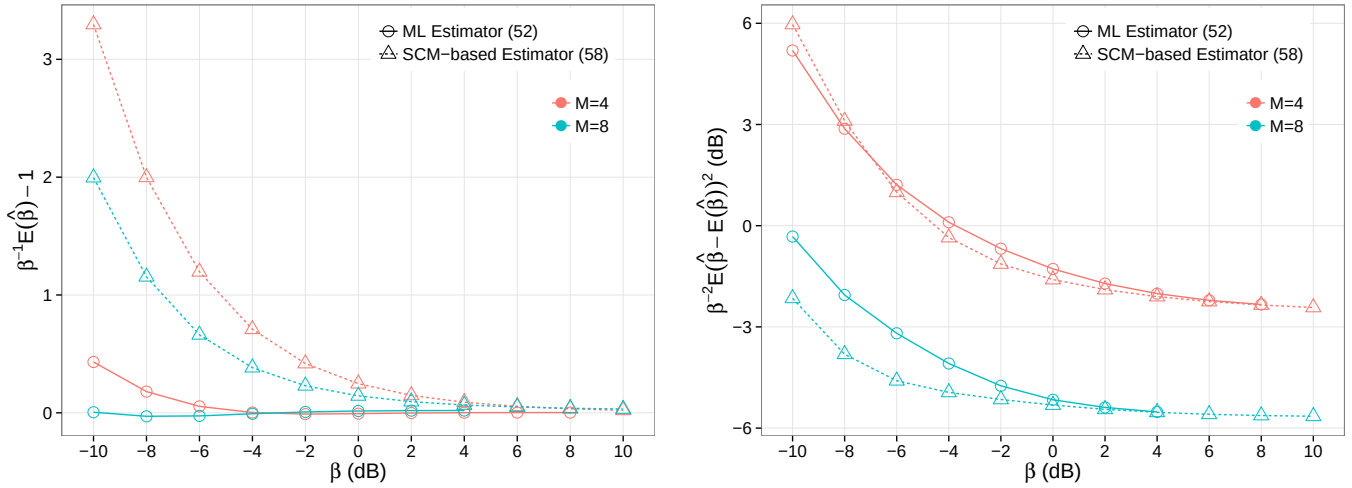

Fig. 3. Relative bias (left figure) and relative error variance (right figure) of the ML and SCM-based UL channel gain estimators, as a function of the channel gain β for $Q = 1$. The left figure shows that the ML estimator (solid lines) is unbiased for a sufficiently high number of antennas/observations $M \geq 8$. The SCM-based estimator (dashed lines) is biased for low $\beta = \rho_{\mathrm{U}}$ because the SCM is biased itself for low sample support. In terms of relative error variance, both estimators exhibit similar performance, which improves for an increasing number of antennas/observations M.

and DL subspace estimators, and demonstrated the asymptotic efficiency of the SVD-based estimators by means of Monte Carlo simulations. Since the inverse FIM relies on truncated Taylor expansions, the formulated CRBs hold only for small perturbations; that is, their range of validity is lower bounded by $\rho_{\mathrm{U}} > 0$dB and $\rho_{\mathrm{D}} > 10\mathrm{lg}(M)$dB.

In addition, we have discussed several possibilities for the reduction of the processing complexity. For the case $\tau/M = 1$, the order of the pilot reverse modulation and the SVD-based DL subspace estimator can be swapped without any performance penalties, which turns a matrix-matrix multiplication into a matrix-vector multiplication. For the UL subspace estimation with $\tau/M = 1$, the pilot reverse modulation can be completely omitted. Moreover, the SVD computation, which has generally a cubic time complexity, can be replaced by the power iteration method. As shown by our simulations, the number of iterations can be kept constant with respect to the number of antennas M, which implies a quadratic time complexity.

Finally, we formulated the ML estimator for the UL channel gain, which relies on the knowledge of the repeater's average transmit power and the UL perturbation variance. The resulting likelihood function, however, does not admit a closed-form solution for its maximum, so that we have to resort to a numerical line search method. As shown by the numerical experiments, this ML estimator is robust against strong perturbations (i.e., it is unbiased for a sufficiently large number of antennas/observations), but is numerically unstable for large M and ρ_{U}. Therefore, we propose a simple SCM-based estimator, which is naturally biased for a small sample

support (i.e., small values of M), but exhibits a similar relative error variance as the ML estimator.

In the following, we briefly discuss some open research questions.

1) ML Estimation for Nonwhite Perturbations: In [10], the case of correlated noise with a known covariance matrix is discussed. In our UL model (5), this corresponds to a perturbation matrix $\tilde{\boldsymbol{N}} = [\tilde{\boldsymbol{n}}_1, \ldots, \tilde{\boldsymbol{n}}_\tau]$ with i.i.d. columns, each following $\mathcal{CN}(\boldsymbol{0}_M, \boldsymbol{R}_{\tilde{\boldsymbol{n}}})$, where $\boldsymbol{R}_{\tilde{\boldsymbol{n}}} = \mathrm{E}[\tilde{\boldsymbol{n}}_t \tilde{\boldsymbol{n}}_t^H], \forall t$ denotes the $M \times M$ covariance matrix of the transformed perturbations. Note that this covariance model admits only sensible interpretations for $\tau/M = 1$, because then we have $\boldsymbol{R}_{\tilde{\boldsymbol{n}}} = \mathrm{E}[\boldsymbol{n}_t \boldsymbol{\Phi}\boldsymbol{\Phi}^H \boldsymbol{n}_t^H] = \mathrm{E}[\boldsymbol{n}_t \boldsymbol{n}_t^H], \forall t$; that is, we observe temporally independent (w.r.t. the index t) but spatially correlated perturbations $\boldsymbol{N} = [\boldsymbol{n}_1, \ldots, \boldsymbol{n}_\tau]$ in (3).

For nonwhite noise, the simple SVD-based estimator in (43) is biased by the principal invariant subspace of $\boldsymbol{R}_{\tilde{\boldsymbol{n}}}$. Therefore, a whitened SVD-based approach is proposed

$$\boldsymbol{R}_{\tilde{\boldsymbol{n}}}^{-1/2} \tilde{\boldsymbol{Y}} := \boldsymbol{U}\boldsymbol{\Sigma}\boldsymbol{V}^H, \tag{62}$$

where the ML estimate for $\boldsymbol{g}$ is given by $\boldsymbol{g}^{\mathrm{ML}} \sim \boldsymbol{R}_{\tilde{\boldsymbol{n}}}^{1/2} \boldsymbol{u}_1$.

One should note that this spatial covariance model for the UL perturbations implies 'temporally' correlated UL perturbations for the DL subspace estimator, which violates our model assumption even for the asymptotic case $\rho_{\mathrm{D}} \to \infty$.

2) Bayesian Subspace Estimation: A Bayesian subspace estimation approach is described in [17], which is applicable to our UL subspace estimation for the case $\tau/M = 1$ (i.e., the elements of $\boldsymbol{x}$ in (3) must be i.i.d.). The resulting estimator is called minimum mean square distance (MMSD) subspace estimator because the MSE in (22) is adopted as the cost function. A closed-form solution is derived for the Bingham distribution [11] as the pior for $\boldsymbol{g}$, given by

$$\pi(\boldsymbol{g}) \propto \mathrm{etr}\{\kappa \boldsymbol{g}^H \boldsymbol{\Pi}\boldsymbol{\Pi}^H \boldsymbol{g}\} \tag{63}$$

where $\boldsymbol{\Pi} \in G_p(\mathbb{C}^M)$ reflects the prior knowledge about the p-dimensional subspace where $\boldsymbol{g}$ evolves, and κ is a concentration parameter: the larger κ the more concentrated around $\boldsymbol{\Pi}$ is the subspace of $\boldsymbol{g}$.

The MMSD estimate $\boldsymbol{g}^{\mathrm{MMSD}}$ is given by the dominant eigenvector of the matrix $(\kappa \boldsymbol{\Pi}\boldsymbol{\Pi}^H + \boldsymbol{Y}\boldsymbol{Y}^H)$. Obviously, the MMSD estimator collapses to the ML estimator for the case of an uniform prior distribution (i.e., when $\boldsymbol{g}$ is isotropically distributed). Unfortunately, a MMSD estimator for the DL subspace cannot be deduced from the results provided in [17].

ACKNOWLEDGMENT

This work has been conducted within Bell Labs' FutureCell project. The authors wish to thank project initiators T. Klein, T. Sizer, A. Pascht and O. Blume. They are also grateful for the helpful comments of V. Suryaprakash.

REFERENCES

[1] T. Marzetta, "Noncooperative cellular wireless with unlimited numbers of base station antennas," *IEEE Transactions on Wireless Communications*, vol. 9, no. 11, pp. 3590–3600, November 2010.

[2] G. Caire, N. Jindal, M. Kobayashi, and N. Ravindran, "Multiuser MIMO achievable rates with downlink training and channel state feedback," *IEEE Trans. Inf. Theory*, vol. 56, no. 6, pp. 2845–2866, June 2010.

[3] T. Marzetta and B. Hochwald, "Fast transfer of channel state information in wireless systems," *IEEE Transactions on Signal Processing*, vol. 54, no. 4, pp. 1268–1278, April 2006.

[4] L. Withers, R. Taylor, and D. Warme, "Echo-MIMO: A two-way channel training method for matched cooperative beamforming," *IEEE Transactions on Signal Processing*, vol. 56, no. 9, pp. 4419–4432, Sept 2008.

[5] D. Samardzija and N. Mandayam, "Unquantized and uncoded channel state information feedback in multiple-antenna multiuser systems," *IEEE Transactions on Communications*, vol. 54, no. 7, pp. 1335–1345, July 2006.

[6] J. Choi, D. Love, and P. Bidigare, "Downlink training techniques for FDD massive MIMO systems: Open-loop and closed-loop training with memory," *IEEE Journal of Selected Topics in Signal Processing*, vol. 8, no. 5, pp. 802–814, Oct 2014.

[7] X. Rao and V. Lau, "Distributed compressive CSIT estimation and feedback for FDD multi-user massive MIMO systems," *IEEE Transactions on Signal Processing*, vol. 62, no. 12, pp. 3261–3271, June 2014.

[8] T. L. Marzetta, O. Blume, P. Rulikowski, S. Maier, A. Pascht, and T. Klein, "Frequency division duplex (fdd) massive mimo backhaul for repeater small cells," Patent US 2 016 134 438 (A1), May 12, 2016.

[9] L. Ahumada, R. Feick, R. A. Valenzuela, and C. Morales, "Measurement and characterization of the temporal behavior of fixed wireless links," *IEEE Transactions on Vehicular Technology*, vol. 54, no. 6, pp. 1913–1922, Nov 2005.

[10] S. Smith, "Covariance, subspace, and intrinsic cramer-rao bounds," *Signal Processing, IEEE Transactions on*, vol. 53, no. 5, pp. 1610–1630, May 2005.

[11] J. T. Kent, "The complex bingham distribution and shape analysis," *Journal of the Royal Statistical Society, Series B (Methodological)*, vol. 56, no. 2, 1994.

[12] N. O'Donoughue and J. M. F. Moura, "On the product of independent complex gaussians," *IEEE Transactions on Signal Processing*, vol. 60, no. 3, pp. 1050–1063, March 2012.

[13] G. Golub and C. Van Loan, *Matrix Computations*, 2nd ed. Baltimore: Johns Hopkins University Press, 1989.

[14] T. L. Marzetta and B. M. Hochwald, "Capacity of a mobile multiple-antenna communication link in rayleigh flat fading," *IEEE Transactions on Information Theory*, vol. 45, pp. 139–157, 1999.

[15] D. Bertsekas, *Nonlinear Programming*. Athena Scientific, 1995.

[16] N. Boumal, "On intrinsic cramér-rao bounds for riemannian submanifolds and quotient manifolds," *IEEE Transactions on Signal Processing*, vol. 61, no. 7, pp. 1809–1821, April 2013.

[17] O. Besson, N. Dobigeon, and J.-Y. Tourneret, "Minimum mean square distance estimation of a subspace," *Signal Processing, IEEE Transactions on*, vol. 59, no. 12, pp. 5709–5720, Dec 2011.